

1

2 **Soil infiltration characteristics and pore distribution under**

3 **freezing-thawing conditions**

4 **Ruiqi Jiang^{1,2,3,*}, Tianxiao Li^{1,2,3,*}, Dong Liu^{1,2,3,*}, Qiang Fu^{1,2,3,*}, Renjie Hou^{1,2,3},**

5 **Qinglin Li¹, Song Cui^{1,2,3}, Mo Li^{1,2,3}**

6 ¹ School of Water Conservancy & Civil Engineering, Northeast Agricultural University, Harbin 150030,

7 China

8 ² Key Laboratory of Effective Utilization of Agricultural Water Resources of Ministry of Agriculture,

9 Northeast Agricultural University, Harbin, Heilongjiang 150030, China

10 ³ Heilongjiang Provincial Key Laboratory of Water Resources and Water Conservancy Engineering in Cold

11 Region, Northeast Agricultural University, Harbin, Heilongjiang 150030, China

12 *** Dong Liu and Qiang Fu are corresponding authors.**

13 **★ These authors contributed equally to this work.**

14 *Corresponding author at: School of Water Conservancy and Civil Engineering, Northeast Agricultural

15 University, Harbin, Heilongjiang 150030, China

16 *Correspondence to:* liudong9599@yeah.net (Dong Liu). fuqiang0629@126.com (Qiang Fu)

17 **Abstract.** Frozen soil infiltration widely occurs in hydrological processes such as seasonal soil freezing and

18 thawing, snowmelt infiltration, and runoff. Accurate measurement and simulation of parameters related to

19 frozen soil infiltration processes are highly important for agricultural water management, environmental

20 issues and engineering problems in cold regions. Temperature changes cause soil pore size distribution

21 variations and consequently dynamic infiltration capacity changes during different freeze-thaw periods. To

22 better understand these complex processes and to reveal the freeze-thaw action effects on soil pore

23 distribution and infiltration capacity, black soils, meadow soils and chernozem were selected as test subjects,

24 these soil types account for the largest arable land area in Heilongjiang Province, China. Laboratory tests of
25 soils at different temperatures were conducted using a tension infiltrometer and ethylene glycol aqueous
26 solution. The stable infiltration rate and hydraulic conductivity were measured, and the soil pore distribution
27 was calculated. The results indicated that for the different soil types, macropores, which constituted
28 approximately 0.1% to 0.2% of the soil volume under unfrozen conditions, contributed approximately 50%
29 of the saturated flow, and after soil freezing, the soil macropore proportion decreased to 0.05% to 0.1%,
30 while the saturated flow proportion decreased to approximately 30%. Soil moisture froze into ice crystals
31 inside relatively large pores, resulting in numerous smaller-sized pores, which reduced the number of
32 macropores but increased the number of smaller-sized mesopores, so that the frozen soil infiltration capacity
33 was no longer solely dependent on the macropores. After the ice crystals had melted, more pores were formed
34 within the soil, enhancing the soil permeability.

35 **Key words:** Freezing-thawing soil; Hydraulic conductivity; Pore distribution; Macropores; Infiltration
36 characteristics

37 **1 Introduction**

38 Over the last few decades, the temperature changes caused by global warming have altered the freezing state
39 of near-surface soils, and in China, changes in characteristic values such as the extent of the mean annual
40 area of the seasonal soil freeze/thaw state and maximum freezing depth, indicate the degradation of frozen
41 soil, especially at high latitudes (Wang et al., 2019; Peng et al., 2016). Under the effect of temperature, most
42 frozen regions experience seasonal freezing and thawing of soil, accompanied by coupled soil water and
43 heat movement as well as frost heave processes, thus making the soil structure and function more variable
44 (Oztas and Fayetorbay, 2003; Fu et al., 2019; Gao et al., 2018). Parameters such as the soil infiltration rate
45 and hydraulic conductivity are key factors in the study of soil water movement, groundwater recharge, and

46 solute and contaminant transport simulation (Angulo-Jaramillo et al., 2000). In regard to unfrozen soils,
47 temperature has been shown to change the soil structure and kinematic viscosity of soil water, thereby
48 affecting the unsaturated hydraulic conductivity of soils (Gao and Shao, 2015). In terms of frozen soils, the
49 water infiltration characteristics and pore size distribution are highly variable and difficult to observe
50 (Watanabe et al., 2013); moreover, the water movement in freezing-thawing soils is complicated by the
51 migration of water and heat and the associated water phase change (Jarvis et al., 2016;Hayashi, 2013). The
52 accurate measurement of water movement parameters and soil pore distribution under freeze-thaw
53 conditions is a necessary prerequisite for the quantitative description of the water movement in frozen soil,
54 and the mechanism and degree of influence of the temperature on the infiltration rate, hydraulic conductivity,
55 porosity and other parameters in the different stages of freeze-thaw periods require further research.

56 Currently, quantitative studies of the infiltration process in freezing-thawing soils can be mainly divided into
57 experimental and model studies. Field experiments have been performed less often because under natural
58 conditions, infiltration water exhibits a preferential flow into the deep soil, and the alternating freeze-thaw
59 effect forms ice crystals to block the flow path through large pores, subsequently limiting water infiltration
60 (Daniel et al., 1997), while the melting effect of the infiltration water on ice makes it difficult to reach a
61 steady infiltration state. Therefore, the current relevant achievements are mainly focused on the infiltration
62 process of snowmelt water (Hayashi et al., 2003) and the influence of preferential flow (Mohammed et al.,
63 2019). Controlled laboratory experiments provide new opportunities for the simulation of frozen soil
64 infiltration processes and the measurement of infiltration parameters. Williams and Burt (1974) conducted
65 early direct measurements in the laboratory, resolved the water freezing problem by adding lactose and
66 applied dialysis membranes on both sides of soil columns, and they determined the water conductivity of
67 saturated specimens in the horizontal direction (Burt and Williams, 1976). Andersland et al. (1996) measured

68 the hydraulic conductivity of frozen granular soils at different saturations using a conventional drop
69 permeameter with decane as the permeant and concluded that the hydraulic conductivity was the same as
70 that of unfrozen soils with water as the infiltration solution. McCauley et al. (2002) determined and compared
71 the differences in hydraulic conductivity, permeability and infiltration rate between frozen and unfrozen soils
72 using diesel mixtures as permeants, and their results indicated that the ice content determines whether soil is
73 sufficiently impermeable. Zhao et al. (2013) quantified the unsaturated hydraulic conductivity of frozen soil
74 using antifreeze instead of water, [and](#) adopted a multistage outflow method under controlled pressures [in](#)
75 [combination with the concept of](#) ~~and introduced~~ the pore impedance coefficient (Jame and Norum, 1980).
76 However, most of these studies did not consider the differences in kinematic viscosity and surface tension
77 between soil water and other solutions, which often results in an overestimation of hydraulic conductivity,
78 and homemade devices in the laboratory are often inconvenient for generalization in the field. Due to the
79 dynamic changes in the temperature and moisture phase, direct measurement is difficult, and hydraulic
80 conductivity empirical equations and models of frozen soil have been developed. First, the frozen soil
81 hydraulic conductivity was simply considered to follow a power exponential relationship with the
82 temperature (Nixon, 1991; Smith, 1985), while others considered the hydraulic conductivity of frozen soil to
83 be equal to that of unfrozen soil at the same water content and assumed that the hydraulic conductivity of
84 frozen soil was a function of the moisture content of unfrozen soil (Lundin, 1990; Flerchinger and Saxton,
85 1989; Harlan, 1973). On the basis of Campbell's model (Campbell, 1985), Tarnawski and Wagner (1996)
86 proposed a frozen soil hydraulic conductivity model based on the soil particle size distribution and porosity.
87 Watanabe and Wake (2008) viewed soil pores as cylindrical capillaries and suggested that ice formation
88 occurs at the center of these capillaries and established a model to describe the movement of thin film water
89 and capillary water in frozen soil based on the theory of capillaries and surface absorption (Watanabe and

90 Flury, 2008). The similarity between freezing and soil moisture profiles has been demonstrated (Spaans and
91 Baker, 1996;Spaans, 1994), and subsequently, soil freezing characteristic curves have been applied to
92 estimate the unsaturated hydraulic conductivity of frozen soils (Azmatch et al., 2012), which has been
93 combined with field tests and inversion models to achieve a high accuracy (Cheng et al., 2019).

94 Understanding the distribution characteristics of the soil pore system is essential for the evaluation of the
95 water and heat movement processes in soil. Soil macroporosity has been shown to impose a major impact
96 on water cycle processes such as infiltration, nutrient movement and surface runoff. (Demand et al.,
97 2019;Jarvis, 2007). Macroporosity is widespread in a variety of soils and produces preferential flow in both
98 frozen and unfrozen soils (Mohammed et al., 2018;Beven and Germann, 2013), and the pre-freeze moisture
99 conditions affect the amount and state of ice in the macropores of frozen soils, resulting in notable variability
100 in the infiltration capacity of thawed soils (Hayashi et al., 2003;Granger et al., 1984). Field experiments on
101 frozen soil have also demonstrated that macropores accelerate the infiltration rate (Stähli et al., 2004;Kamp
102 et al., 2003), the number and size of macropores affect the freezing and infiltration capacity of soil layers to
103 different extents, and low temperatures cause infiltration water to refreeze inside macropores (Watanabe and
104 Kugisaki, 2017;Stadler et al., 2000). Research on frozen soil macroporosity has largely focused on the
105 qualitative analysis of its impact on the soil structure and infiltration capacity, and with the development of
106 experimental techniques, certain new methods and techniques, such as computed tomography (CT) and X-
107 ray scanning, have been applied to measure the number and distribution of macropores (Taina et al.,
108 2013;Bodhinayake et al., 2004;Grevers et al., 1989), but the lack of sampling techniques targeting frozen
109 soil still restricts related research.

110 Many limitations and deficiencies remain in the direct measurement of frozen soil infiltration characteristics
111 and pore distribution, and the relevant models also require a large amount of measured data to meet the

112 accuracy and applicability requirements. In this paper, the stable infiltration rate and hydraulic conductivity
113 of three types of soils at different temperatures were measured by precise control of the soil and ambient
114 temperatures, and the macropore and mesopore size distribution was calculated by using a tension
115 infiltrometer and a glycol aqueous solution as the infiltration medium. The conclusions provide a basis and
116 reference for the numerical simulation of the coupled water-heat migration process of freezing-thawing soil
117 and related parameterization studies.

118 **2 Materials and methods**

119 **2.1 Test plan**

120 Referring to arable land area data of various regions of Heilongjiang Province, the three types of soils that
121 dominate the cultivated land area in this province are black soils, meadow soils and chernozem (Bureau,
122 1992). Harbin, Zhaoyuan and Zhaozhou were selected as typical soil areas for sampling. A 5-cm surface
123 layer of floating soil and leaves was removed, and topsoil samples were collected at depths ranging from 0-
124 20 cm. After natural air drying and artificial crushing, the soil was sieved, and particles larger than 2 mm in
125 diameter were removed. The remainder was used to prepare soil columns. The basic physical and chemical
126 parameters of the test soils, such as the bulk density, organic content and mechanical parameters, are listed
127 in Table 1.

128 An artificial climate chamber was applied to control the temperature of the soil column and infiltration
129 solution, and four temperature treatments were established with three replications for each treatment: 15°C,
130 unfrozen soil, representing the soil before freezing, which was recorded as 15°C (BF); -5°C, stable freezing;
131 -10°C, stable freezing; and freezing at -10°C followed by thawing at 15°C, representing the soil after melting,
132 which was recorded as 15°C (AM). Each soil column was tested for only one treatment. The freezing and
133 thawing times were both 48 h. When the soil temperature was consistent with the set temperature in the

134 climate chamber, the samples were considered to be completely frozen, and the effect of the number of
 135 freezing and thawing cycles was not considered in this test. According to the basic information of the original
 136 soil, the volumetric moisture content of the sieved soil was set to $30\% \pm 2\%$ using deionized water, with a
 137 dry bulk density of 1.2 g/cm^3 . To reduce the inhomogeneous distribution of soil moisture, a spray bottle was
 138 used to add water to the sieved and air-dried soil in small but repeated amounts, while the change in soil
 139 moisture was detected using sensors, so that the moisture content of the soil columns was controlled within
 140 the set range and the texture was uniform, as well as making the pre-freeze moisture content relatively
 141 consistent between different soil columns. The soil porosity and pre-freezing soil water content of the
 142 repacked samples are shown in Table 2.

143 **Table 1**
 144 **Basic physical and chemical properties of three kinds of soils**

Soil types	Bulk density (g/cm^3)	Organic content (g/kg)	Electrical conductivity (s/m)	Particle size (sand- silt-clay) (%)	Soil texture
Black soil	1.31	28.32	0.02	12.64-70.82-16.54	
Meadow soil	1.22	16.51	0.01	9.52-73.00-17.48	silt loam
Chernozem	1.15	26.52	0.01	38.99-50.30-10.71	

145 **Table 2**
 146 **Soil porosity and pre-freezing soil water content of repacked samples**

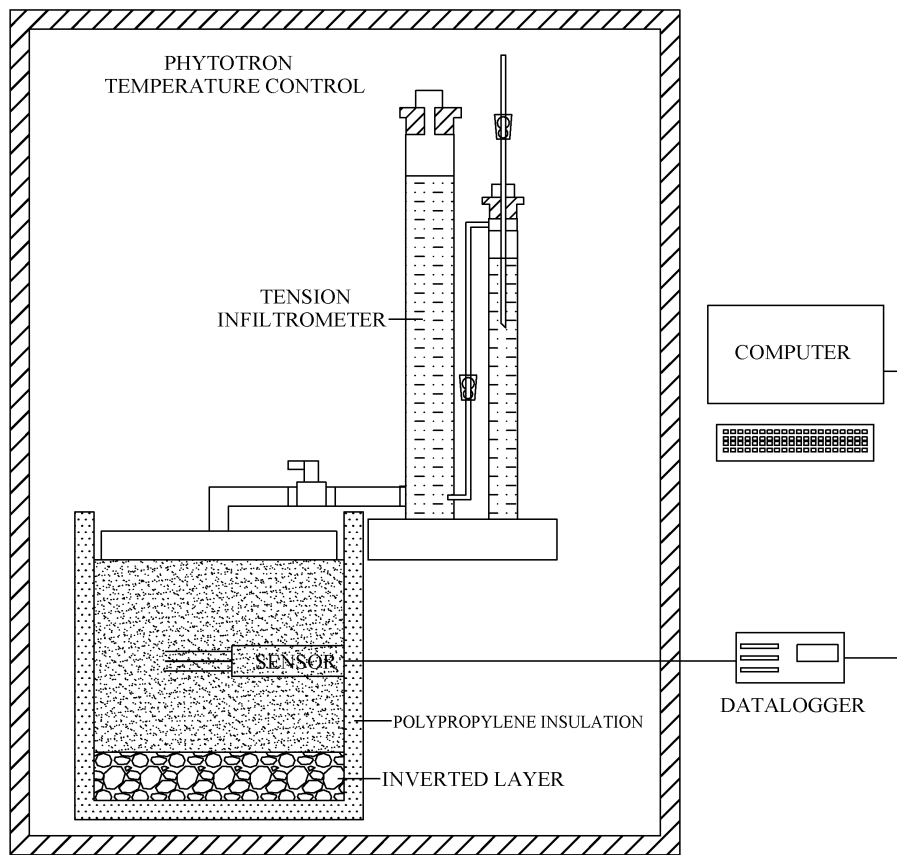
Soil types	Soil porosity (%)	Pre-freezing water content (%)	
		-5°C	-10°C
Black soil	52.76	30.53	29.27
Meadow soil	52.82	29.83	30.70

Chernozem	53.22	30.07	30.93
-----------	-------	-------	-------

147 To ensure a homogeneous column, the soil was loaded into a polyvinyl chloride (PVC) cylinder at 5-cm
148 depth intervals, and petroleum jelly was applied to the sides to reduce the sidewall flow (Lewis and Sjöström,
149 2010). The PVC cylinder was 26 cm in diameter and 30 cm in height, with a perforated plate at the bottom.
150 To prevent lateral seepage, the barrel occurred 5 cm above the soil surface, and the thickness of the soil layer
151 was 20 cm. A HYDRA-PROBE II sensor (STEVENS Water Monitoring Systems, Inc., Portland, Oregon,
152 USA) was inserted in the middle of the barrel to observe the potential soil temperature and liquid water
153 content change to determine whether ice melting occurred, and the ice content of frozen soil was measured
154 by the drying method. A 5-cm thick layer of sand and gravel was placed below the soil column, and a 5-cm
155 thick layer of black polypropylene insulation cotton was wrapped around the outer layer and the bottom of
156 the soil column. The stable infiltration rate under tension levels of -3, -5, -7, -9, -11, and -13 cm was measured
157 with a tension infiltrometer, and the infiltration time and cumulative infiltration were recorded. The detailed
158 layout of the test apparatus is shown in Fig. 1.

159 The addition of a certain amount of lactose, antifreeze or other substances to water greatly reduces the
160 freezing point of water (Zhao et al., 2013; Williams and Burt, 1974) so that the soil macropores are not
161 quickly filled with ice with decreasing temperature, thereby maintaining better conditions for water flow. To
162 further verify the feasibility of the use of deionized water to prepare an aqueous solution of ethylene glycol
163 at a mass concentration of 40% as the infiltration medium for the frozen soil measurements, the surface
164 tension of the aqueous glycol solution at -5°C and -10°C and its relationship with the temperature were
165 measured with a contact angle measuring instrument (OCA20, DataPhysics Instruments, Germany) and a
166 surface tension measuring instrument (DCAT-21, DataPhysics Instruments, Germany), respectively. As an
167 example, the contact angle measurement process of the black soil at -10°C with the aqueous ethylene glycol
168 solution is shown in Fig. 2, and it is observed that the contact angle decreases to 0° within a few seconds

169 after the liquid droplet is placed on the soil, and the liquid droplet completely dissolves in the frozen soil,
 170 which implies that the addition of glycol to water does not alter the wetting ability of the soil particles (Lu
 171 and Likos, 2004). For the unfrozen soils of the 15°C (BF) and 15°C (AM) treatments, deionized water was
 172 used as the infiltration solution, and for the frozen soils of the -5°C and -10°C treatments, aqueous ethylene
 173 glycol solution was used as the infiltration solution. The relevant physicochemical properties of the aqueous
 174 ethylene glycol solution and water are compared in Table 3.



175
 176

Fig. 1. Diagram of the test equipment.



177
 178
 179

Fig. 2. Process of the contact angle measurement between the aqueous ethylene glycol solution and black soil at -10°C.

180 **Table 3**

181 **Comparison of the physicochemical properties of the 40% ethylene glycol aqueous solution and**

182 **water**

Infiltration solution	Temperature (°C)	Density (g/cm ³)	Dynamic viscosity (mPa·s)	Surface tension (mN/m)	Contact angle (°)
Water	15	0.9991	1.14	73.56	0
Ethylene glycol	-5	1.0683	7.18	48.89	0
aqueous solution	-10	1.0696	9.06	49.10	0

183 **2.2 Measurement of the frozen soil hydraulic conductivity**

184 Gardner (1958) proposed that the unsaturated hydraulic conductivity of soil varies with the matric potential

185 as follows:

$$186 \quad K(h) = K_{sat} \exp(\alpha h) \quad (1)$$

187 where K_{sat} is the saturated hydraulic conductivity, cm/hour, and h is the matric potential or tension, cm H₂O.

188 Wooding (1968) considered that the steady-state unconfined infiltration rate into soil from a circular water

189 source of radius R can be calculated with the following equation:

$$190 \quad Q = \pi R^2 K \left[1 + \frac{4}{\pi R \alpha} \right] \quad (2)$$

191 where Q is the amount of water entering the soil per unit time, cm³/h; K is the hydraulic conductivity,

192 cm/hour; and α is a constant. Ankeny et al. (1991) proposed that implementing two successively applied

193 pressure heads h_1 and h_2 could yield the unsaturated hydraulic conductivity, and upon replacing K in Eq. (2)

194 with Eq. (1), the following is obtained:

$$195 \quad Q(h_1) = \pi R^2 K_{sat} \exp(\alpha h_1) \left[1 + \frac{4}{\pi R \alpha} \right] \quad (3)$$

196
$$Q(h_2) = \pi R^2 K_{sat} \exp(\alpha h_2) \left[1 + \frac{4}{\pi R \alpha} \right] \quad (4)$$

197 Dividing Eq. (4) by Eq. (3) and solving for α yields:

198
$$\alpha = \frac{\ln[Q(h_2)/Q(h_1)]}{h_2 - h_1} \quad (5)$$

199 where $Q(h_1)$ and $Q(h_2)$ can be measured, h_1 and h_2 are the preset tension values, and α can be calculated with
 200 Eq. (5). The result can be substituted into Eq. (3) or (4) to calculate K_{sat} . When the number of tension levels
 201 is higher than 2, parameter fitting methods can be applied to improve the accuracy of α and K_{sat} (Hussen and
 202 Warrick, 1993).

203 The tension is controlled by the bubble collecting tube of the tension infiltrometer, and different pressure
 204 heads h correspond to different pore sizes r . By applying different pressure heads h to the soil surface, water
 205 will overcome the surface tension in the corresponding pores and will be discharged, and the infiltration
 206 volume is recorded after reaching the stable infiltration state.

207 Under the assumption that the frozen soil pore ice pressure is equal to the atmospheric pressure and that
 208 solutes are negligible, the Clausius-Clapeyron equation can be adopted to achieve the interconversion
 209 between the soil temperature and suction (Konrad and Morgenstern, 1980; Watanabe et al., 2013), which can
 210 be simplified as follows:

211
$$\psi = -L\rho_w \frac{T}{273.15} \quad (6)$$

212 where ψ is the soil suction, kPa; L is the latent heat of fusion of water, 3.34×10^5 J/kg; ρ_w is the density of
 213 water, 1 g/cm^3 ; and T is the subfreezing temperature, °C. After the unit conversion of the soil suction into h
 214 (cm H_2O), the unsaturated hydraulic conductivity of frozen soil at different negative temperatures can be
 215 obtained via substitution into Eq. (2).

216 **2.3 Measurement of the pore size distribution in frozen soil**

217 As a nonuniform medium, soil consists of pores with various pore sizes, and the equation for the soil pore
218 radius r can be obtained from the capillary model (Watson and Luxmoore, 1986):

$$219 \quad r = -\frac{2\sigma \cos \beta}{\rho gh} \quad (7)$$

220 where σ is the surface tension of the solution, g/s^2 ; β is the contact angle between the solution and pore wall;
221 ρ is the density of the solution, g/cm^3 ; g is the acceleration of gravity, m/s^2 ; and h is the corresponding tension
222 of the tension infiltrometer, $cm H_2O$.

223 The effective macroporosity θ_m can be calculated for various soil particle sizes based on the Poiseuille
224 equation (Wilson and Luxmoore, 1988):

$$225 \quad \theta_m = 8\mu K_m / \rho gr^2 \quad (8)$$

226 where μ is the dynamic viscosity of the fluid, $g/(cm*s)$; K_m is the macropore hydraulic conductivity and is
227 defined as the difference between $K(h)$ at various tension gradients, cm/h ; and r is the corresponding
228 equivalent pore size. The effective porosity is equal to the number of pores per unit area multiplied by the
229 area of the corresponding pore size. For different pore sizes, the maximum number of effective macropores
230 per unit area N can be calculated with the following equation:

$$231 \quad N = \theta_m / \pi r^2 \quad (9)$$

232 where N is the number of effective macropores per unit area, and Eq. (7) calculates the minimum value of
233 the pore radius, while the result obtained with Eq. (9) is actually the maximum number of effective
234 macropores per unit area and the maximum porosity.

235 Considering the differences in surface tension and density between the aqueous ethylene glycol solution and
236 water, when calculating the frozen soil pore size distribution, it is necessary to convert the tension into the
237 equivalent pore radius according to Eq. (7), which is classified and subdivided into large and medium pores
238 according to the common classification method (Luxmoore, 1981), the details of which are listed in Table 4,

239 while the corresponding tension values in Table 4 are substituted into the fitting curve equation to calculate
 240 the corresponding stable infiltration rate q and unsaturated hydraulic conductivity K .

241 **Table 4**

242 **Tension and equivalent pore radius conversions**

Pore types	Pore radius (mm)	Tension conversion (cm)		
		Water (15°C)	Ethylene glycol aqueous solution (- 5°C)	Ethylene glycol aqueous solution (- 10°C)
Macroporous	>0.5	0~3	0~1.86	0~1.87
	0.3-0.5	3~5	1.86~3.11	1.86~3.12
Mesoporous	0.15-0.3	5~10	3.11~6.22	3.12~6.23
	0.1-0.15	10~15	6.22~9.32	6.23~9.35
	0.05-0.1	15~30	9.32~18.65	9.35~18.70

243 **3 Results**

244 **3.1 Infiltration characteristics of freezing-thawing soils**

245 Curves of the recorded cumulative infiltration and infiltration rate were plotted over time, as shown in Figs.
 246 3 and 4, respectively. The unfrozen water contents and ice contents of the frozen samples are shown in Table
 247 5. The constant α and saturated hydraulic conductivity K_{sat} were calculated under different tensions h and
 248 corresponding steady-state infiltration rates q , and the unsaturated hydraulic conductivity under different
 249 tensions was calculated with Eq. (1). The stable infiltration rate and unsaturated hydraulic conductivity at
 250 different temperatures are shown in Fig. 5, and the details of α and K_{sat} are listed in Table 6.

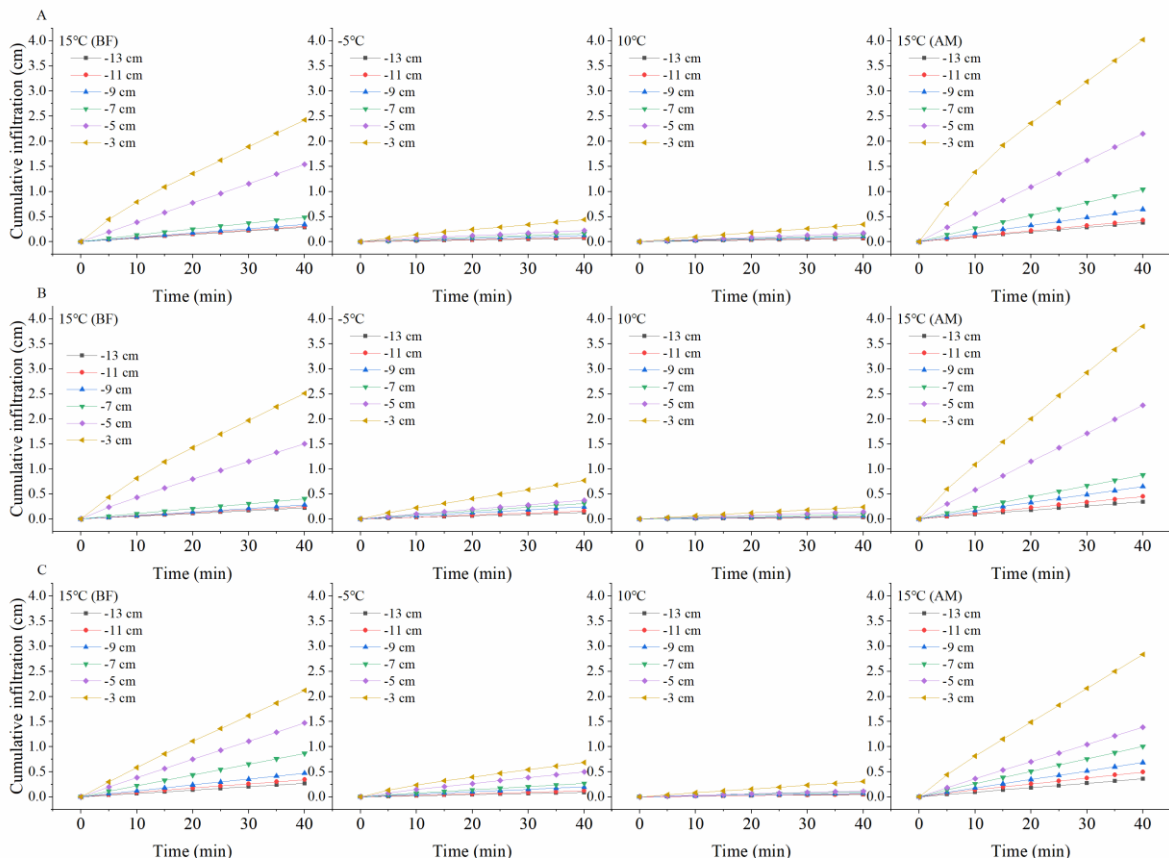
251 **Table 5**

252 **Unfrozen water contents and ice contents of the frozen samples**

Soil types	Unfrozen water contents (cm ³ /cm ³)		Ice contents (cm ³ /cm ³)	
	-5°C	-10°C	-5°C	-10°C
Black soil	0.123	0.101	0.159	0.179
Meadow soil	0.128	0.109	0.145	0.167
Chernozem	0.119	0.097	0.151	0.185

253

254

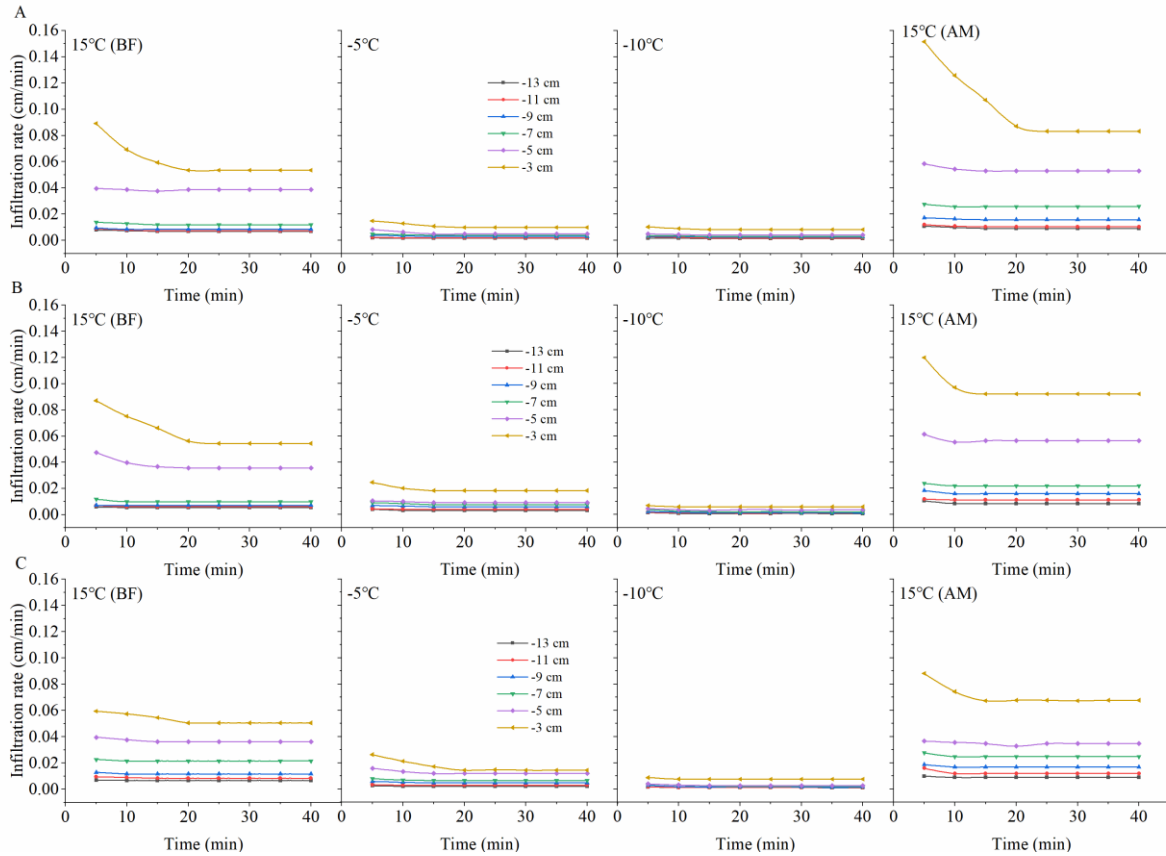


255

256 **Fig. 3.** Cumulative infiltration over time under the different treatments.

257 Note: A Black Soil; B Meadow Soil; C Chernozem.

258



259

260 **Fig. 4.** Infiltration rate over time under the different treatments.

261 Note: A Black Soil; B Meadow Soil; C Chernozem.

262 As shown in Figs. 4 and 5, under the different tension conditions, the infiltration capacity of the unfrozen

263 soil is basically consistent with the findings of field experiments and is highly influenced by the tension

264 value (Wang et al., 1998). Compared to the room-temperature soil, the cumulative infiltration of frozen soil

265 slowly increases, and the infiltration rate always remains low, while under the same negative temperature

266 treatment, the influence of the tension value is also greatly reduced. When the temperature was reduced to -

267 10°C, few major tension differences were observed except for the maximum tension of -3 cm. Based on the

268 change in the slope of the two curves, the time for the unfrozen soil to reach the stable infiltration rate usually

269 ranges from 15~20 min, while the time for the frozen soil to reach the stable infiltration rate is usually 10

270 min under higher tensions of -3 and -5 cm and 5 min under lower tensions. A comparison of the infiltration

271 process before and after the freezing and thawing of the soil indicates that overall, the cumulative infiltration

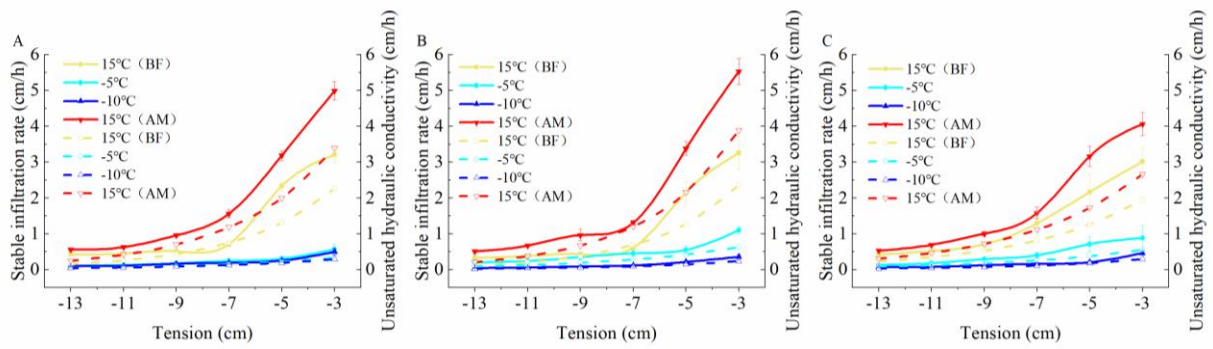
272 and infiltration rate exhibited varying degrees of increase with increasing tension value, and the increase
 273 amplitude expanded. Moreover, the difference in the cumulative infiltration and infiltration rate between the
 274 low tension levels ranging from -9 to -13 cm after soil thawing was larger than that before soil freezing,
 275 which also indirectly demonstrated that freezing and thawing could further stabilize the soil pore distribution
 276 by affecting the homogeneity, which will be detailed in subsequent sections.

277 **Table 6**

278 **Infiltration parameters of the different temperature treatments of the three soil types**

Soil types	Temperature (°C)	α (cm/h)	K_{sat} (cm/h)	Permeability (m²)
Black soil	15 (BF)	0.2742	5.1480	1.66E-09
	-5	0.1993	0.5960	1.14E-09
	-10	0.2028	0.5221	1.25E-09
	15 (AM)	0.2629	7.4658	2.41E-09
Meadow soil	15 (BF)	0.3071	5.9232	1.92E-09
	-5	0.1996	1.1385	2.17E-09
	-10	0.2477	0.4903	1.18E-09
	15 (AM)	0.2934	9.3757	3.03E-09
Chernozem	15 (BF)	0.2166	3.7185	1.20E-09
	-5	0.1907	0.9739	1.86E-09
	-10	0.2508	0.6077	1.46E-09
	15 (AM)	0.2182	5.1283	1.66E-09

279



280

281 **Fig. 5.** Variation curves of the unsaturated hydraulic conductivity and stable infiltration rate with the

282 tension for the different treatments of the three soils.

283 Note: A Black soil; B meadow soil; C chernozem. The solid lines represent the stable infiltration rate, and

284 the dashed lines represent the unsaturated hydraulic conductivity.

285 By combining Fig. 5 and Table 6, we observe that the three types of soils exhibit a high infiltration capacity

286 under normal temperature conditions. With increasing set tension value, the suction force of the soil matrix

287 gradually weakened, the constraint and maintenance capacity of the matric potential with respect to the soil

288 water decreased, the number of pores involved in the soil water infiltration process increased, and the

289 unsaturated hydraulic conductivity and stable infiltration rate of the three types of soils exhibited different

290 degrees of increase. When the temperature was lowered from 15°C to -5°C and remained constant for a

291 certain time, ~~and~~ the soil reached the stable frozen state which usually indicated that there were no more

292 drastic changes in temperature and moisture content, the saturated water conductivity of the black soil,

293 meadow soil and chernozem soil decreased by 88.42%, 80.78% and 73.8%, respectively. When the soil

294 temperature was decreased to -10 °C, due to the presence of liquid water in the pores, the saturated water

295 conductivity still exhibited a certain decrease over the pre-freeze conditions and continued to decrease by

296 1.43%, 10.94% and 9.85%, respectively. At negative temperatures, the unsaturated hydraulic conductivity

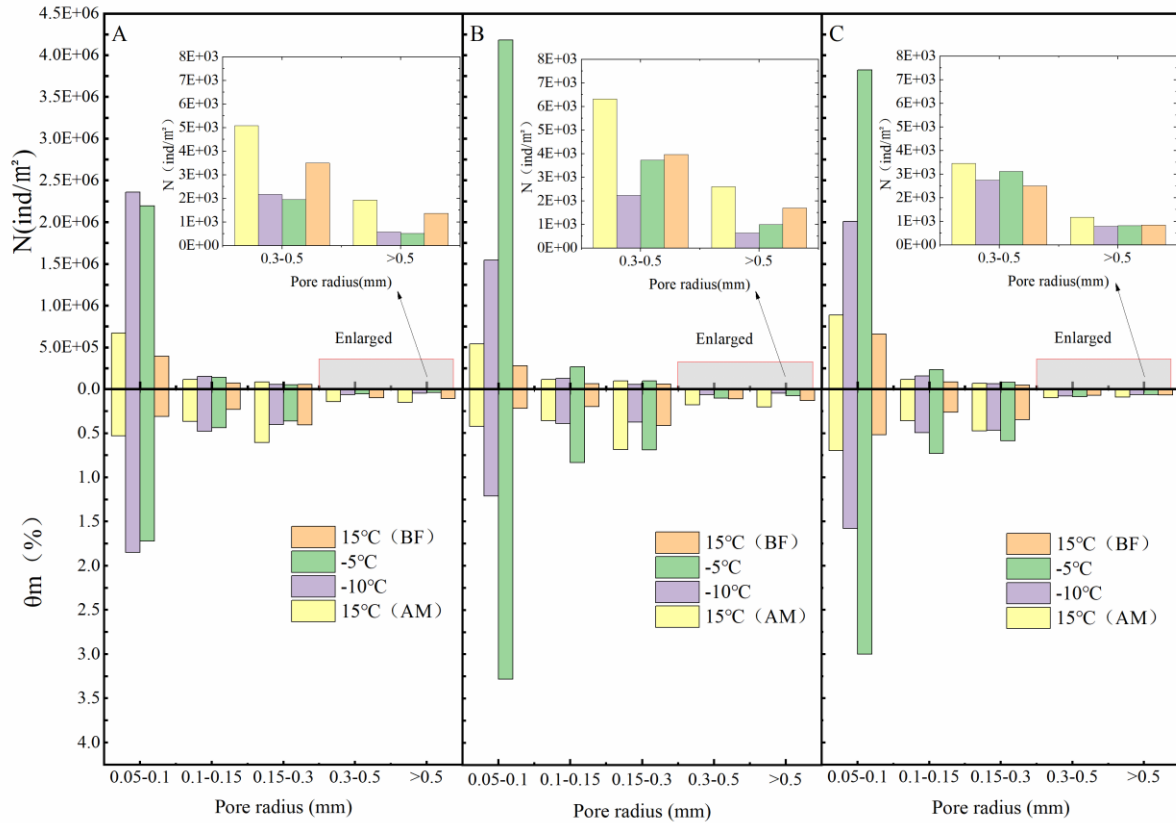
297 decreased considerably and fluctuated within a small range, mainly because the unfrozen water content and

298 saturated hydraulic conductivity were low after soil freezing. Based on a comparing of the -5°C and -10°C

299 treatments, the unsaturated hydraulic conductivity (ANOVA, $P=0.72$, $F=0.14$) and stable infiltration rate
300 (ANOVA, $P=0.71$, $F=0.15$) of the black soil exhibited almost no significant change, indicating that most of
301 its pores were filled with ice crystals at -5°C and were no longer involved in water infiltration. The
302 unsaturated water conductivity of the meadow and chernozem soils still exhibited a more significant
303 reduction when the freezing temperature was further reduced to -10°C . When the temperature was raised
304 again to 15°C and the soil was completely thawed, the steady infiltration rate and saturated hydraulic
305 conductivity increased with increasing temperature, and the values were higher than those of the soil at the
306 same temperature before freezing. The saturated hydraulic conductivity of the black soil, meadow soil and
307 chernozem increased by 45.02%, 58.63% and 37.91%, respectively, relative to the 15°C (BF) treatment
308 values.

309 **3.2 Pore distribution characteristics of the freezing-thawing soil**

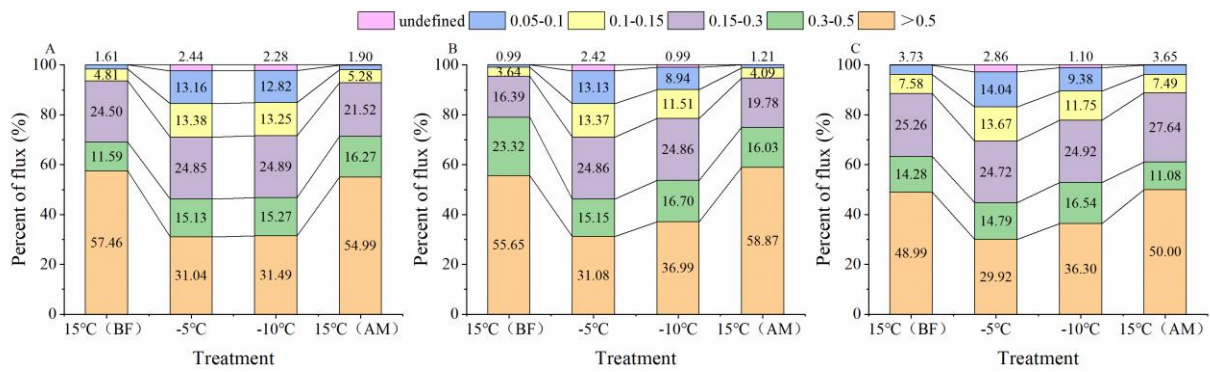
310 Considering the differences in the physical and chemical properties between the infiltration solutions,
311 infiltration parameters such as the hydraulic conductivity and stable infiltration rate alone do not fully reflect
312 the infiltration characteristics and internal pore size of frozen soils. According to Eqs. (7)-(9), the maximum
313 number per unit area N , effective porosity θ_m and percentage of pore flow to saturated flow P corresponding
314 to the different soil pore sizes of the three soils under the different temperature treatments were calculated,
315 as shown in Figs. 6 and 7.



316

317 **Fig. 6.** Number of pores and effective porosity of the different equivalent pores.

318 Note: A Black Soil; B Meadow Soil; C Chernozem.



319

320 **Fig. 7.** Percentage of the pore flow in the saturated flow for the different equivalent pore sizes.

321 Note: A Black Soil; B Meadow Soil; C Chernozem.

322 Fig. 6 shows that pores of different equivalent radii widely occur in all three soils, and under all four

323 temperature treatments, the largest N value is that for the medium pores with an equivalent radius of 0.05-

324 0.1 mm, and N gradually decreases with increasing equivalent radius size. Under the two room-temperature

325 treatments at 15°C (BF) and 15°C (AM), the largest number of 0.05- to 0.1-mm medium pores and the
326 smallest number of >0.5-mm macropores differed by two orders of magnitude, and the number of pores of
327 each size exhibited different degrees of increase or decrease in the two treatments at -5°C and -10°C where
328 freezing occurred, with the number of medium pores with an equivalent pore size of 0.05-0.1 mm
329 significantly changing. Increases of more than an order of magnitude were achieved in all three soils, while
330 the macropores with an equivalent pore size of >0.5 mm were generally reduced by an order of magnitude,
331 with the difference in the number of pores of these two sizes reaching four orders of magnitude. This
332 indicates that freezing caused by temperature change significantly alters the soil internal structure, with ice
333 crystals forming in the relatively large pores containing the internal soil moisture, resulting in a large number
334 of smaller pores. Based on an assessment of the two treatments at -5°C and -10°C separately, when the
335 temperature was lowered from -5°C to -10°C, the number of pores in each pore size interval of the meadow
336 and chernozem soils exhibited a significant decrease, while the black soil revealed a small increase, which
337 might be related to the high organic matter content of the black soil. A comparison of the two treatments at
338 15°C (BF) and 15°C (AM) indicated that the number of pores in all three soils increased to different degrees
339 after thawing, and more pores were formed with the melting of ice crystals after the freeze-thaw destruction
340 of the soil particles, which enhanced the soil water conductivity.

341 Comprehensive analysis of Figs. 6 and 7 reveals that before freezing, the θ_m values of the various pore sizes
342 of the black soils, meadow soils and chernozem with an equivalent radius of >0.5 mm were 0.11%, 0.13%
343 and 0.07%, respectively, while the P value reached 57.46%, 55.65% and 48.99%, respectively, with the
344 values of the thawed soil similar to these values. This indicates that for all five soil pore sizes under unfrozen
345 conditions, although the number of macropores with a pore size >0.5 mm was the smallest and the effective
346 porosity was the lowest, their contribution to the saturated flow was usually more than half, and the

347 macropores needed to represent only a small fraction of the pore volume to significantly contribute to the
348 soil water flow. For the frozen soil, the P value of the >0.5-mm macropores was significantly reduced and
349 remained at approximately 30% after the reduction, while the P value of the smaller pore sizes such as 0.15-
350 0.3 mm, 0.1-0.15 mm, and 0.05-0.1 mm, revealed different degrees of increase. Moreover, the smaller the
351 pore size, the greater the P value increased, and the contribution of these pores eventually accounted for
352 more than 10% of the saturated flow. The saturated flow became more evenly distributed across the pores of
353 each size, and the total proportion of medium pores exceeded that of the macropores. This indicates that the
354 freezing action caused obvious changes to the soil structure, pore size and quantity, and although the
355 macropores still played an important role, the infiltration capacity of the frozen soil no longer relied solely
356 on these macropores, and the contribution of certain smaller-sized mesopores to the infiltration capacity of
357 the frozen soil could no longer be neglected. Selecting black soil as an example, the total effective porosity
358 of the pores of each size under the four treatments was 1.15%, 2.62%, 2.84%, and 1.80%, and the P values
359 were 99.97%, 97.56%, 97.72%, and 99.96%, respectively, which implies that the soil water infiltrated almost
360 entirely via the large and medium pores. The small micropores, even in large numbers, contributed little to
361 the infiltration process.

362 **4 Discussion**

363 **4.1 Permeability and hydraulic conductivity of the frozen soil**

364 It is worth noting that the theory underpinning the tension infiltration analysis in this article is based on the
365 assumption that larger pores only flow fully saturated which means no air-water interface inside the pore and
366 excludes the formation of an air-water interface with flowing water in larger pores (Perroux and White, 1988).
367 However, recent work has shown that this flow mode does indeed occur (Beven and Germann, 2013; Nimmo,
368 2012, 2010). [In addition, in unfrozen tension infiltrometer experiments, the soil moisture is assumed to be](#)

369 [that imposed by the applied tension, whereas in the experiments with frozen samples, the applied tension is](#)
370 [assumed to affect only the pores that are active during infiltration.](#)

371 In the field environment, although it is difficult to accurately measure the infiltration rate of frozen soils
372 using traditional instruments and methods such as single-loop infiltrators, the obtained test results still
373 demonstrate that the infiltration capacity decreases by one or more orders of magnitude when the soil is
374 frozen (Stähli et al., 2004). Although the cumulative infiltration and infiltration rate of frozen soil are low,
375 the presence of unfrozen water allows a certain amount of infiltration flow to be maintained in the soil. When
376 water is applied as the infiltration solution, the low temperature of the frozen soil easily causes the infiltration
377 water to freeze, thus forming a thin layer of ice on the soil particle surface and delaying the subsequent
378 infiltration of water. This phenomenon results in a low infiltration rate after the freezing of soils with a high
379 initial water content and a relatively high infiltration rate after the freezing of dry soils (Watanabe et al.,
380 2013), because the higher the ice content is, the more latent heat needs to be overcome to melt any ice crystals,
381 resulting in a weakened propagation of the melting front, thus limiting the infiltration rate so that it is
382 controlled by the downward movement of the melting leading edge of the ice crystals (Pittman et al., 2020).
383 During the measurements using the tension infiltrator in this study, the sensor temperature always remained
384 consistent with the soil temperature, indicating that the use of an aqueous glycol solution could be a useful
385 way to avoid the problem of freezing of the infiltration solution. In addition, the hydraulic conductivity of
386 frozen soils with different capacities and at various water flow rates was demonstrated not to greatly differ
387 (Watanabe and Osada, 2017).

388 Whether water or other low-freezing point solutions are applied as infiltration media, the hydraulic
389 conductivity of frozen soil significantly changes only within a limited temperature range above -0.5°C
390 depending on the unfrozen water and ice contents, and at a soil temperature below -0.5°C , the hydraulic

391 conductivity usually decreases to less than 10^{-10} m/s (Watanabe and Osada, 2017; Williams and Burt, 1974).
392 The unsaturated hydraulic conductivity in our experiments was measured at a set tension level, and according
393 to Eq. (6), the soil substrate potential increases by 125 m for every 1°C decrease in temperature (Williams
394 and Smith, 1989), while the frozen soil hydraulic conductivity calculated at -5°C and -10°C, which
395 corresponds to the actual matric potential, is much lower than 10^{-10} m/s, close to the zero point of the
396 unsaturated hydraulic conductivity variation curves in Fig. 5, and can be ignored. This suggests that even
397 under ideal conditions where no heat exchange occurs between the infiltration solution and the soil and no
398 freezing of the infiltration water takes place to prevent subsequent infiltration, the unsaturated hydraulic
399 conductivity of frozen soil is so low that the frozen soil at lower temperatures in its natural state could be
400 considered impermeable, with respect to both water and other solutions. It should also be noted that we used
401 different liquids at different temperatures and that the difference in infiltration parameters such as K_{sat} with
402 temperature is related to the different viscosities of the liquid. It is predictable that if water is also used in
403 frozen soils, such differences will be relatively insignificant as the ice melts.

404 **4.2 Effect of freeze-thaw cycles on soil pore distribution**

405 In our study, the N value after freezing for the different types of soil was approximately 1000-2000/m² base
406 on the tension infiltrator, which agreed well with other studies such as conventional soil ring methods
407 (Pittman et al., 2020) or geophysical imaging techniques such as X-ray and CT (Ding et al., 2019; Holten et
408 al., 2018), and remained at ~~a~~ the same magnitude ~~(Pittman et al., 2020)~~, indicating that the method is generally
409 reliable. Compared with saturated frozen soils (Ding et al., 2019), the effect of freeze-thaw cycles on the
410 pore distribution of unsaturated frozen soil is also significant. Moreover, it should be noted that instruments
411 such as CT are usually expensive and difficult to carry, tension infiltrators are affordable and widely used,
412 and combined with temperature control equipment, they will be helpful for field measurements of

413 [macroporosity in frozen soils](#). The freeze-thaw effect significantly improves the water conductivity of the
414 different types of soils because it increases the porosity, decreases the soil compactness and dry weight, and
415 thus increases the soil water conductivity (Fouli et al., 2013). On this basis, we also found that the freeze/thaw
416 process significantly altered the size and number of soil pores, especially after freezing, and the number of
417 macropores decreased, while the contribution of macropores to the saturated flow decreased. The proportion
418 of the saturated flow in the mesopores with a pore size of <0.3 mm approached or even exceeded the
419 proportion in the macropores, indicating that the soil water inside relatively large pores is more likely to
420 freeze, which in turn creates a large number of small pores, whereas the water transfer process in unfrozen
421 soils primarily relies on the macropores, with obvious differences (Wilson and Luxmoore, 1988; Watson and
422 Luxmoore, 1986). The unsaturated water conductivity of the frozen soils measured in this study was quite
423 low, but under human control (Watanabe and Kugisaki, 2017) or natural conditions in the field (Espeby,
424 1990), water has been shown to infiltrate frozen soils through macropores as long as the pore size is large
425 enough. Considering that the soil in this experiment was disturbed soil that had been air dried and sieved,
426 although the macropores created by tillage practices (Lipiec et al., 2006) and invertebrate activities (Lavelle
427 et al., 2006) were excluded, due to the inherent heterogeneity of the soil particles, macropores remain in the
428 uniformly filled soil column (Cortis and Berkowitz, 2004; Oswald et al., 1997), and these macropores still
429 played a role in determining the infiltration water flow. [In addition, according to the equations of \$N\$ and \$\theta_m\$,](#)
430 [it can be found that the main source of their uncertainty is the value of the pore radius \$r\$, and Eq. \(7\)](#)
431 [calculates the minimum value of pore radius, while the result obtained with Eq. \(9\) is in fact the upper limit](#)
432 [of effective macropores per unit area and effective porosity, which may also lead to a certain overestimation.](#)
433 [Furthermore, freezing of water may also have a potential effect on the microstructure of soil pores](#)(Wan and
434 Yang, 2020).

435 There are still only a few studies related to frozen soil macropore flow and pore distribution; consequently,
436 more data should be acquired, and more models should be developed to better understand water movement
437 in frozen soil regions. The experiments in this paper are based on repacked soils that were subjected to the
438 first freeze-thaw cycle in the laboratory, and the conclusions may not be comprehensive. In subsequent
439 studies, we will consider applying the methods used in this paper to field experiments to examine the
440 dynamics of the infiltration capacity and pore distribution in nonhomogeneous soils during whole freeze-
441 thaw periods under real outdoor climatic conditions, such as lower temperatures and more severe freeze-
442 thaw cycles, but the infiltration solution must be carefully selected; as ethylene glycol has low toxicity, to
443 prevent contamination of agricultural soils and crops, a certain concentration of lactose could be considered
444 (Burt and Williams, 1976; Williams and Burt, 1974). At room temperature, an ethylene glycol aqueous
445 solution and water have similar densities and relatively similar viscosities. We have compared these two
446 infiltration solutions in unfrozen soil field experiments, and the infiltration and pore conditions were
447 basically similar, so we still used an aqueous glycol solution in the frozen soil laboratory experiment.
448 Measurements should focus on frozen soil layers at different depths, especially in the vicinity of freezing
449 peaks, and the spatial variability in the distribution of frozen soil pores should be investigated. This work
450 helps to improve the accuracy of simulations such as those of frozen soil water and heat movement or
451 snowmelt water infiltration processes.

452 **5 Conclusions**

453 In this paper, the infiltration capacity of soil columns under four temperature treatments representing various
454 freeze-thaw stages was measured, and the distribution of the pores of various sizes within the soil was
455 calculated based on the measurements by applying an aqueous ethylene glycol solution with a tension
456 infiltrator in the laboratory. The results revealed that for the three types of soils, i.e., black soil, meadow soil

457 and chernozem, the macropores, which accounted for only approximately 0.1% to 0.2% of the soil volume
458 at room temperature, contributed approximately 50% to the saturated flow, and after freezing, the proportion
459 of macropores decreased to 0.05% to 0.1%, while their share of the saturated flow decreased to
460 approximately 30%. Coupled with the even smaller mesopores, the large and medium pores, accounting for
461 approximately 1% to 2% of the soil volume, conducted almost all of the soil moisture under saturated
462 conditions. Freezing decreased the number of macropores and increased the number of smaller-sized
463 mesopores, thereby significantly increasing their contribution to the frozen soil infiltration capacity so that
464 the latter was no longer solely dependent on the macropores. The infiltration parameters and pore distribution
465 of the black soil were the least affected by the different negative freezing temperatures under the same
466 moisture content and weight capacity conditions, while those of the meadow soil were the most impacted.

467 **Data availability**

468 Data used in this study are available at Figshare (doi: [10.6084/m9.figshare.12965123](https://doi.org/10.6084/m9.figshare.12965123)).

469 **Author contributions**

470 Ruiqi Jiang designed the research program. Tianxiao Li and Ruiqi Jiang built and deployed the soil column
471 and instruments with assistance from Qinglin Li and Renjie Hou. Dong Liu and Qiang Fu provided funding
472 for test equipment. Song Cui collected soil samples in the field. Ruiqi Jiang and Tianxiao Li analyzed the
473 laboratory data. Ruiqi Jiang prepared the manuscript with comments from Tianxiao Li and Dong Liu.

474 **Competing interests**

475 The authors declare that they have no conflicts of interest

476 **Acknowledgements**

477 We acknowledge that this research was supported by the National Natural Science Foundation of China
478 (51679039), the National Science Fund for Distinguished Young Scholars (51825901), the Heilongjiang

479 Provincial Science Fund for Distinguished Young Scholars (YQ2020E002),"Young Talents" Project of
480 Northeast Agricultural University(18QC28), and the China Postdoctoral Science Foundation Grant
481 (2019M651247).

482 **References**

- 483 Andersland, O. B., Wiggert, D. C., and Davies, S. H.: Hydraulic conductivity of frozen granular soils, *J*
484 *Environ Eng*, 122, 212-216, 10.1061/(ASCE)0733-9372(1996)122:3(212), 1996.
- 485 Angulo-Jaramillo, R., Vandervaere, J.-P., Roulier, S., Thony, J.-L., Gaudet, J.-P., and Vauclin, M.: Field
486 measurement of soil surface hydraulic properties by disc and ring infiltrometers: A review and recent
487 developments, *Soil and Tillage Research*, 55, 1-29, 10.1016/S0167-1987(00)00098-2, 2000.
- 488 Ankeny, M. D., Ahmed, M., Kaspar, T. C., and Horton, R.: Simple field method for determining
489 unsaturated hydraulic conductivity, *Soil Sci Soc Am J*, 55, 467-470,
490 10.2136/sssaj1991.03615995005500020028x, 1991.
- 491 Azmatch, T. F., Sego, D. C., Arenson, L. U., and Biggar, K. W.: Using soil freezing characteristic curve to
492 estimate the hydraulic conductivity function of partially frozen soils, *Cold Reg. Sci. Technol*, 83, 103-109,
493 10.1016/j.coldregions.2012.07.002, 2012.
- 494 Beven, K., and Germann, P.: Macropores and water flow in soils revisited, *Water Resour Res*, 49, 3071-
495 3092, 10.1002/wrcr.20156, 2013.
- 496 Bodhinayake, W., Si, B. C., and Xiao, C.: New method for determining water - conducting macro - and
497 mesoporosity from tension infiltrometer, *Soil Sci Soc Am J*, 68, 760-769, 10.2136/sssaj2004.0760, 2004.
- 498 Bureau, H. L. A.: Heilongjiang soil, Agriculture Press, Beijing, 1992.
- 499 Burt, T., and Williams, P. J.: Hydraulic conductivity in frozen soils, *Earth Surface Processes*, 1, 349-360,
500 10.1002/esp.3290010404, 1976.
- 501 Campbell, G. S.: Soil physics with BASIC: transport models for soil-plant systems, Elsevier, Amsterdam,
502 1985.
- 503 Cheng, Q., Xu, Q., Cheng, X., Yu, S., Wang, Z., Sun, Y., Yan, X., and Jones, S. B.: In-situ estimation of
504 unsaturated hydraulic conductivity in freezing soil using improved field data and inverse numerical modeling,
505 *Agr Forest Meteorol*, 279, 107746, 10.1016/j.agrformet.2019.107746, 2019.
- 506 Cortis, A., and Berkowitz, B.: Anomalous transport in "classical" soil and sand columns, *Soil Sci Soc Am*
507 *J*, 68, 1539-1548, 10.2136/sssaj2004.1539, 2004.
- 508 Daniel, Stadler, and, Hannes, Flühler, and, Per-Erik, and Jansson: Modelling vertical and lateral water flow
509 in frozen and sloped forest soil plots, *Cold Regions Science & Technology*, 10.1016/S0165-232X(97)00017-7,
510 1997.
- 511 Demand, D., Selker, J. S., and Weiler, M.: Influences of macropores on infiltration into seasonally frozen
512 soil, *Vadose Zone J*, 18, 1-14, 10.2136/vzj2018.08.0147, 2019.
- 513 Ding, B., Rezanezhad, F., Gharedaghloo, B., Cappellen, P. V., and Passeport, E.: Bioretention cells under
514 cold climate conditions: Effects of freezing and thawing on water infiltration, soil structure, and nutrient
515 removal, *Sci Total Environ*, 649, 2019.
- 516 Espeby, B.: Tracing the origin of natural waters in a glacial till slope during snowmelt, *J Hydrol*, 118, 107-
517 127, 10.1016/0022-1694(90)90253-T, 1990.
- 518 Flerchinger, G. N., and Saxton, K. E.: Simultaneous Heat and Water Model of a Freezing Snow-Residue-

519 Soil System I. Theory and Development, American Society of Agricultural Engineers, 10.13031/2013.31041,
520 1989.

521 Fouli, Y., Cade-Menun, B. J., and Cutforth, H. W.: Freeze–thaw cycles and soil water content effects on
522 infiltration rate of three Saskatchewan soils, *Can J Soil Sci*, 93, 485-496, 10.4141/CJSS2012-060, 2013.

523 Fu, Q., Zhao, H., Li, T., Hou, R., Liu, D., Ji, Y., Zhou, Z., and Yang, L.: Effects of biochar addition on soil
524 hydraulic properties before and after freezing-thawing, *Catena*, 176, 112-124, 10.1016/j.catena.2019.01.008,
525 2019.

526 Gao, B., Yang, D., Qin, Y., Wang, Y., Li, H., Zhang, Y., and Zhang, T.: Change in frozen soils and its effect
527 on regional hydrology, upper Heihe basin, northeastern Qinghai-Tibetan Plateau, *Cryosphere*, 12, 657-673,
528 2018.

529 Gao, H., and Shao, M.: Effects of temperature changes on soil hydraulic properties, *Soil Till Res*, 153,
530 10.1016/j.still.2015.05.003, 2015.

531 Gardner, W.: Some steady-state solutions of the unsaturated moisture flow equation with application to
532 evaporation from a water table, *Soil Sci*, 85, 228-232, 10.1097/00010694-195804000-00006, 1958.

533 Granger, R. J., Gray, D. M., and Dyck, G. E.: Snowmelt infiltration to frozen Prairie soils, *Can J Earth Sci*,
534 21, 669-677, 10.1139/e84-073, 1984.

535 Grevers, M., JONG, E. D., and St. Arnaud, R.: The characterization of soil macroporosity with CT
536 scanning, *Can J Soil Sci*, 69, 629-637, 10.4141/cjss89-062, 1989.

537 Harlan, R.: Analysis of coupled heat - fluid transport in partially frozen soil, *Water Resour Res*, 9, 1314-
538 1323, 10.1029/WR009i005p01314, 1973.

539 Hayashi, M., Kamp, G. V. D., and Schmidt, R.: Focused infiltration of snowmelt water in partially frozen
540 soil under small depressions, *J Hydrol*, 270, 214-229, 10.1016/S0022-1694(02)00287-1, 2003.

541 Hayashi, M.: The Cold Vadose Zone: Hydrological and Ecological Significance of Frozen-Soil Processes,
542 *Vadose Zone J*, 12, 10.2136/vzj2013.03.0064, 2013.

543 Holten, R., Be, F. N., Almvik, M., Katuwal, S., and Eklo, O. M.: The effect of freezing and thawing on
544 water flow and MCPA leaching in partially frozen soil, *J Contam Hydrol*, 219, 72-85, 2018.

545 Hussien, A., and Warrick, A.: Alternative analyses of hydraulic data from disc tension infiltrometers, *Water*
546 *Resour Res*, 29, 4103-4108, 10.1029/93WR02404, 1993.

547 Jame, Y. W., and Norum, D. I.: Heat and mass transfer in a freezing unsaturated porous medium, *Water*
548 *Resour Res*, 16, 811–819, 1980.

549 Jarvis, N.: A review of non - equilibrium water flow and solute transport in soil macropores: Principles,
550 controlling factors and consequences for water quality, *Eur J Soil Sci*, 58, 523-546, 10.1111/j.1365-
551 2389.2007.00915.x, 2007.

552 Jarvis, N., Koestel, J., and Larsbo, M.: Understanding Preferential Flow in the Vadose Zone: Recent
553 Advances and Future Prospects, *Vadose Zone J*, 15, 10.2136/vzj2016.09.0075, 2016.

554 Kamp, G. v. d., Hayashi, M., and Gallén, D.: Comparing the hydrology of grassed and cultivated
555 catchments in the semi-arid Canadian prairies, *Hydrol Process*, 10.1002/hyp.1157, 2003.

556 Konrad, J.-M., and Morgenstern, N. R.: A mechanistic theory of ice lens formation in fine-grained soils,
557 *Can Geotech J*, 17, 473-486, 10.1139/t80-056, 1980.

558 Lavelle, P., Decaëns, T., Aubert, M., Barot, S. b., Blouin, M., Bureau, F., Margerie, P., Mora, P., and Rossi,
559 J.-P.: Soil invertebrates and ecosystem services, *Eur J Soil Biol*, 42, S3-S15, 10.1016/j.ejsobi.2006.10.002, 2006.

560 Lewis, J., and Sjöström, J.: Optimizing the experimental design of soil columns in saturated and
561 unsaturated transport experiments, *J Contam Hydrol*, 115, 1-13, 2010.

562 Lipiec, J., Kuś, J., Słowińska-Jurkiewicz, A., and Nosalewicz, A.: Soil porosity and water infiltration as

563 influenced by tillage methods, *Soil and Tillage research*, 89, 210-220, 10.1016/j.still.2005.07.012, 2006.

564 Lu, N., and Likos, W. J.: *Unsaturated soil mechanics*, Wiley, Hoboken, 2004.

565 Lundin, L.-C.: Hydraulic properties in an operational model of frozen soil, *J Hydrol*, 118, 289-310,

566 10.1016/0022-1694(90)90264-X, 1990.

567 Luxmoore, R.: Micro-, meso-, and macroporosity of soil, *Soil Sci Soc Am J*, 45, 671-672,

568 10.2136/sssaj1981.03615995004500030051x, 1981.

569 McCauley, C. A., White, D. M., Lilly, M. R., and Nyman, D. M.: A comparison of hydraulic conductivities,

570 permeabilities and infiltration rates in frozen and unfrozen soils, *Cold Reg. Sci. Technol*, 34, 117-125,

571 10.1016/S0165-232X(01)00064-7, 2002.

572 Mohammed, A. A., Kurylyk, B. L., Cey, E. E., and Hayashi, M.: Snowmelt infiltration and macropore flow

573 in frozen soils: Overview, knowledge gaps, and a conceptual framework, *Vadose Zone J*, 17, 1-15,

574 10.2136/vzj2018.04.0084, 2018.

575 Mohammed, A. A., Pavlovskii, I., Cey, E. E., and Hayashi, M.: Effects of preferential flow on snowmelt

576 partitioning and groundwater recharge in frozen soils, *Hydrol Earth Syst Sc*, 23, 5017-5031, 10.5194/hess-23-

577 5017-2019, 2019.

578 Nimmo, J. R.: Theory for Source-Responsive and Free-Surface Film Modeling of Unsaturated Flow,

579 *Vadose Zone J*, 9, 295-306, 10.2136/vzj2009.0085, 2010.

580 Nimmo, J. R.: Preferential flow occurs in unsaturated conditions, *Hydrol Process*, 26, 786-789,

581 10.1002/hyp.8380, 2012.

582 Nixon, J.: Discrete ice lens theory for frost heave in soils, *Can Geotech J*, 28, 843-859, 10.1139/t91-102,

583 1991.

584 Oswald, S., Kinzelbach, W., Greiner, A., and Brix, G.: Observation of flow and transport processes in

585 artificial porous media via magnetic resonance imaging in three dimensions, *Geoderma*, 80, 417-429,

586 10.1016/S0016-7061(97)00064-5, 1997.

587 Oztas, T., and Fayetorbay, F.: Effect of freezing and thawing processes on soil aggregate stability, *Catena*,

588 52, 1-8, 10.1016/S0341-8162(02)00177-7, 2003.

589 Peng, X., Frauenfeld, O. W., Cao, B., Wang, K., Wang, H., Su, H., Huang, Z., Yue, D., and Zhang, T.:

590 Response of changes in seasonal soil freeze/thaw state to climate change from 1950 to 2010 across china,

591 *Journal of Geophysical Research Earth Surface*, 10.1002/2016JF003876, 2016.

592 Perroux, K. M., and White, I.: Designs for Disc Permeameters, *Soil Sci Soc Am J*, 52, 1205-1215,

593 10.2136/sssaj1988.03615995005200050001x, 1988.

594 Pittman, F., Mohammed, A., and Cey, E.: Effects of antecedent moisture and macroporosity on infiltration

595 and water flow in frozen soil, *Hydrol Process*, 34, 795-809, 10.1002/hyp.13629, 2020.

596 Smith, M.: Observations of soil freezing and frost heave at Inuvik, Northwest Territories, Canada, *Can J*

597 *Earth Sci*, 22, 283-290, 10.1016/0148-9062(85)90073-7, 1985.

598 Spaans, E. J.: The soil freezing characteristic: Its measurement and similarity to the soil moisture

599 characteristic, 1994.

600 Spaans, E. J., and Baker, J. M.: The soil freezing characteristic: Its measurement and similarity to the soil

601 moisture characteristic, *Soil Sci Soc Am J*, 60, 13-19, 10.2136/sssaj1996.03615995006000010005x, 1996.

602 Stadler, D., Sta" hli, M., Aeby, P., and Flu" hler, H.: Dye tracing and image analysis for quantifying water

603 infiltration into frozen soils, *Soil Sci Soc Am J*, 64, 505-516, 10.2136/sssaj2000.642505x, 2000.

604 St" ahli, M., Bayard, D., Wydler, H., and Fl" uhler, H.: Snowmelt Infiltration into Alpine Soils Visualized by

605 Dye Tracer Technique, *Arctic Antarctic & Alpine Research*, 36, 128-135, 10.1657/1523-

606 0430(2004)036[0128:SIASV]2.0.CO;2, 2004.

607 Taina, I. A., Heck, R. J., Deen, W., and Ma, E. Y.: Quantification of freeze–thaw related structure in
608 cultivated topsoils using X-ray computer tomography, *Can J Soil Sci*, 93, 533-553, 10.4141/CJSS2012-044,
609 2013.

610 Tarnawski, V. R., and Wagner, B.: On the prediction of hydraulic conductivity of frozen soils, *Can Geotech*
611 *J*, 33, 176-180, 10.1139/t96-033, 1996.

612 Wan, X., and Yang, Z. J.: Pore water freezing characteristic in saline soils based on pore size distribution,
613 *Cold Reg. Sci. Technol*, 173, 103030.103031-103030.103012, 2020.

614 Wang, D., Yates, S., and Ernst, F.: Determining soil hydraulic properties using tension infiltrometers, time
615 domain reflectometry, and tensiometers, *Soil Sci Soc Am J*, 62, 318-325,
616 10.2136/sssaj1998.03615995006200020004x 1998.

617 Wang, X., Chen, R., Liu, G., Yang, Y., Song, Y., Liu, J., Liu, Z., Han, C., Liu, X., Guo, S., Wang, L., and
618 Zheng, Q.: Spatial distributions and temporal variations of the near-surface soil freeze state across China under
619 climate change, *Global Planet Change*, 172, 150-158, 10.1016/j.gloplacha.2018.09.016, 2019.

620 Watanabe, K., and Flury, M.: Capillary bundle model of hydraulic conductivity for frozen soil, *Water*
621 *Resour Res*, 44, 10.1029/2008WR007012, 2008.

622 Watanabe, K., and Wake, T.: Hydraulic conductivity in frozen unsaturated soil, *Proceedings of the 9th*
623 *International Conference on Permafrost*, 2008, 1927-1932,

624 Watanabe, K., Kito, T., Dun, S., Wu, J. Q., Greer, R. C., and Flury, M.: Water infiltration into a frozen soil
625 with simultaneous melting of the frozen layer, *Vadose Zone J*, 12, vzj2011.0188, 10.2136/vzj2011.0188, 2013.

626 Watanabe, K., and Kugisaki, Y.: Effect of macropores on soil freezing and thawing with infiltration, *Hydrol*
627 *Process*, 31, 270-278, 10.1002/hyp.10939, 2017.

628 Watanabe, K., and Osada, Y.: Simultaneous measurement of unfrozen water content and hydraulic
629 conductivity of partially frozen soil near 0 C, *Cold Reg. Sci. Technol*, 142, 79-84,
630 10.1016/j.coldregions.2017.08.002, 2017.

631 Watson, K., and Luxmoore, R.: Estimating macroporosity in a forest watershed by use of a tension
632 infiltrometer, *Soil Sci Soc Am J*, 50, 578-582, 10.2136/sssaj1986.03615995005000030007x, 1986.

633 Williams, P., and Burt, T.: Measurement of hydraulic conductivity of frozen soils, *Can Geotech J*, 11, 647-
634 650, 10.1139/t74-066, 1974.

635 Williams, P. J., and Smith, M. W.: *The frozen earth: fundamentals of geocryology*, Cambridge University
636 Press, 1989.

637 Wilson, G., and Luxmoore, R.: Infiltration, macroporosity, and mesoporosity distributions on two forested
638 watersheds, *Soil Sci Soc Am J*, 52, 329-335, 10.2136/sssaj1988.03615995005200020005x, 1988.

639 Wooding, R.: Steady infiltration from a shallow circular pond, *Water Resour Res*, 4, 1259-1273,
640 10.1029/WR004i006p01259, 1968.

641 Zhao, Y., Nishimura, T., Hill, R., and Miyazaki, T.: Determining hydraulic conductivity for air - filled
642 porosity in an unsaturated frozen soil by the multistep outflow method, *Vadose Zone J*, 12, 1-10,
643 10.2136/vzj2012.0061, 2013.

644